Int. J. Nano Dimens., 11 (2): 99-111, Spring 2020

ORIGINAL ARTICLE

Structural, morphological and optical characterization of green synthesized ZnS nanoparticles using Azadirachta Indica (Neem) leaf extract

Subhas Chandra Tudu[1], Maciej Zubko[2, 3], Joachim Kusz [4], Ashis Bhattacharjee [1,]*

[1]*Physics, Visva-Bharati University, Santiniketan –731235, India*
[2] *Institute of Materials Science, University of Silesia, Chorzów, Poland*
[3]*Department of Physics, University of Hradec Králové, Hradec Králové, Czech Republic*
[4]*Institute of Physics, University of Silesia, Katowice, Poland*

Received 01 December 2019; revised 04 January 2020; accepted 06 January 2020; available online 20 January 2020

Abstract

ZnS nanoparticles have been synthesized using various amounts of aqueous Azadirachta Indica (Neem) leaf extract as capping agent and stabilizer. The synthesized nanoparticles were studied by FTIR, powder X-ray diffraction (XRD), scanning electron microscopy (SEM), transmission electron microscopy (TEM), energy dispersive analysis of X-rays (EDAX) and UV-Visible spectroscopy. FTIR spectra shows that the biomolecules such as polyphenols, carboxylic acids, polysaccharide, amino acids and proteins present in the extract are responsible for the binding and stabilizing the synthesized ZnS nanoparticles. Analysis of the XRD data confirms the cubic structure of the synthesized materials with an average particle size of ~2 nm. Using XRD data the microstrain and dislocation density in ZnS crystals have been estimated. The particle size, strain and dislocation density are found to be affected by the amount of the extract used for synthesis. SEM and TEM studies were made to study the morphology and size of the particles. The EDAX spectra confirmed the presence of zinc and sulfur in single nanoparticle. UV-Visible spectra indicated a blue shift in the absorption peak for the extract-capped ZnS materials in comparison to the pure ZnS. The particle size of the ZnS nanoparticles estimated using UV-Visible spectral data along with those obtained from XRD analysis confirms that the green-synthesized ZnS nanoparticles lie in the range of quantum dots. The present study describes a simple, cost effective way of nanoparticle synthesis suitable for large scale production

Keywords: *Green Synthesis; Nanoparticle; Neem Leaf; Physical Characterization; Quantum Dot; Zinc Sulphide.*

How to cite this article

Chandra Tudu S, Zubko M, Kusz J, Bhattacharjee A. Structural, morphological and optical characterization of green synthesized ZnS nanoparticles using Azadirachta Indica (Neem) leaf extract. Int. J. Nano Dimens., 2020; 11 (2): 99-111.

INTRODUCTION

Zinc sulphide (ZnS) is an important semiconductor material belonging to II–VI group with a wide band gap of 3.68 eV which is a leading candidate for various sensing and optoelectronics devices [1-3]. ZnS has two different allotropic forms - zinc blend or sphalerite (cubic) and wurtzite (hexagonal close pack) among which the cubic form has more stable phase at low temperatures. Nanostructured ZnS exhibits distinct properties which are different from its bulk counterpart. Nowadays green synthesis of nanoparticle using biological entities is of great importance due to its nontoxic, cost-effective and eco-friendly nature and best alternative to commonly used conventional methods based on the use of toxic materials evolving toxic products [4]. Green or ecofriendly synthetic methods using plants, their organ extracts and waste products (like peels) instead of using toxic chemicals are available in the literature [5-8]. Recently several reports on the green synthesized ZnS nanoparticle using plants and their products have been reported [9-20]. Green synthesis of ZnS nanoparticle using

* Corresponding Author Email:
ashis.bhattacharjee@visva-bharati.ac.in

Table 1: The sample composition of the NLE-capped ZnS nanomaterials.

Sample name	Sample description	Components using during reaction
A0	Pure ZnS	50 ml of (0.01M) $ZnCl_2$ + 0 ml NLE + 50ml (0.01M) Na_2S
A1	Capped ZnS	50 ml of (0.01M) $ZnCl_2$ + 2.5 ml NLE + 50ml (0.01M) Na_2S
A2	Capped ZnS	50 ml of (0.01M) $ZnCl_2$ + 5 ml NLE + 50ml (0.01M) Na_2S
A3	Capped ZnS	50 ml of (0.01M) $ZnCl_2$ + 7.5 ml NLE + 50ml (0.01M) Na_2S
A4	Capped ZnS	50 ml of (0.01M) $ZnCl_2$ + 10 ml NLE + 50ml (0.01M) Na_2S

leaf extracts has been reported [9-13] whereas Bisauriya *et al.* [14] reported green synthesis of ZnS using environmentally waste banana peel. Honey mediated synthesis of ZnS has been reported for using medicinal purposes [15]. Flower buds have been used for synthesis of ZnS nanoparticle [16]. Multiple species of fungi, like button mushroom (*A. bisporus*) and oyster Mushroom (Pleurotuss ostreatu) [17, 18] and microbes, like *Rhodobacter sphaeroides* [19] and *Klebsiella pneumoniae* [20] have been utilized for growing ZnS nanoparticle of different sizes.

Azadirachta Indica (commonly known as Neem) belongs to the meliaceae family found mostly in different countries in Asia. Each and every part of this tree has the use as either traditional medicine or various clinical applications [21–25]. Neem leaf extract has the antioxidant activity due to presence of mainly phenolic compounds, alkaloids, terpenoids and their derivatives. Terpenoids and flavones are the two main important phytochemicals present in neem which play a vital role in stabilizing the nanoparticle and also act as capping and reducing agent [26]. The use of aqueous neem leaf extract has been in the synthesis of various nanoparticles such as Au, Ag, ZnO etc. [27-29]. In this light, in this paper, we report the green synthesis of ZnS nanoparticles using Neem leaf extract and their structural, morphological and optical properties.

MATERIALS AND METHODS

Chemicals used

Materials used for the synthesis of ZnS nanoparticles are $ZnCl_2$ as a source of Zn^{+2} and Na_2S as a source of S^{-2} and Neem leaf. $ZnCl_2$ and Na_2S are obtained from Loba Chemical Pvt. Ltd, India and used without any further purification.

Preparation of Neem leaf extract

Healthy and fresh leaves of Neem were collected. These were washed rigorously with distilled water to remove the dust and particulate materials attached. After drying the leaves for 10 days in air under cover, they were grinded with mortar and pestle. For preparation of extract, about 25 gm of the Neem leaves dust was taken in a beaker containing 200 ml of distilled water and was then heated up to 70 ˚C and kept for 1 hour until the color of the solution changed to brown. The extract was filtered repeatedly and then stored in refrigerator for further experimental use.

Synthesis of ZnS nanoparticles

ZnS were prepared by green method using Zinc chloride and Sodium sulphide as precursors and Neem leaf extract (NLE) as capping and stabilizing agent. To 50 ml of (0.01M) $ZnCl_2$ aqueous solution, 2.5 ml NLE was added and a homogeneous mixture was obtained under continuous stirring at 70 ˚C. Then 50ml (0.01M) Na_2S solution was added dropwise to this mixture and stirring was contiued further for 1 houruntila white precipitate was formed. This precipitate was filtered off and washed with distilled water repeatedly. Then the filtrate was collected and dried in air at 70 ˚C for 2 hours. The dried sample was powdered by mortar and pestle for characterization. Similarly, few other ZnS samples were synthesized by using different amounts of NLE (5.0, 7.5 and 10ml). Pure ZnS particles were prepared by following the above mentionedmethod without using the NLE. The details of the materials used for syntheses of different ZnS samples are given in Table 1.

Characterization of ZnS nanoparticles

The synthesized ZnS materials were used for physical characterizations like FTIR, powder XRD, SEM, EDAX, TEM and UV-Visible. FTIR study was done with a Perkin Elmer made spectrometer (Analytic 10.4.1) whereas the UV-Visible spectra were taken with a Beckman Coulter made spectrometer (DU 720). Powder XRD study was carried out with Emperian's powder diffractometer equipped with PIXcell^{3D} detector and a Cu-K_α radiation source. Transmission

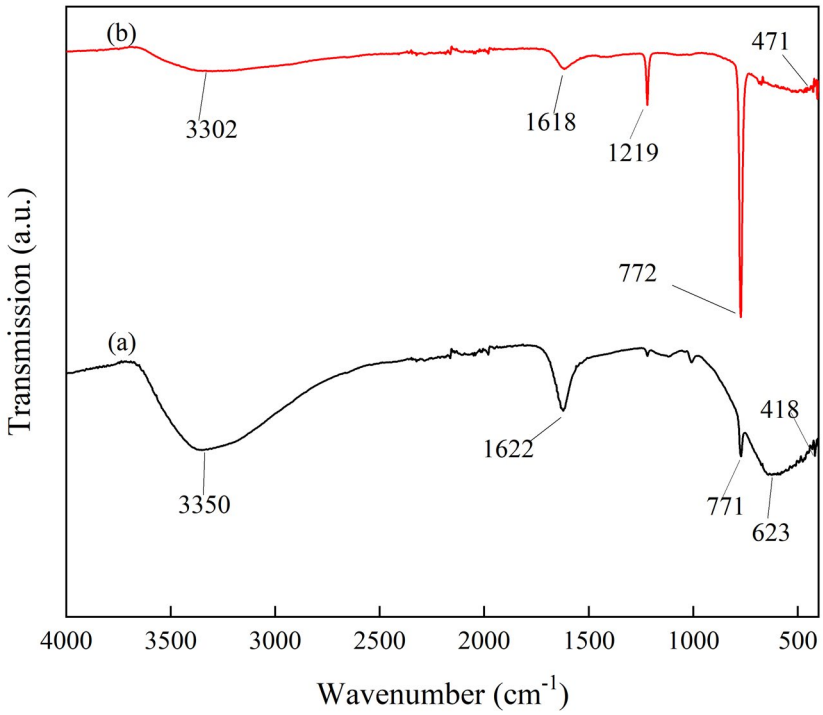

Fig. 1. FTIR spectra: (a) pure ZnS, A0, (b) 10 ml NLE capped ZnS, A4.

Table 2: Position and assignment of absorption bands of ZnS samples observed from FTIR analysis.

Band positions (cm^{-1})					Assignment
A0	A1	A2	A3	A4	
3350.91	3347.65	3285.87	3302.44	3302.34	**O-H** bond
1622.25	1618.37	1614.01	1615.56	1618.19	**N-H** bond
-----	1219.96	1219.93	1219.90	1219.92	**C-N** bond
771.61	772.47	772.51	772.43	772.53	**Zn-S** bond
623.39, 418.53	450.33, 415.7	588.13, 407.59	578.13, 416.33	471.59, 405.90	**Zn-S** stretching

electron microscopy (TEM) observations were performed using a JEOL JEM 3010 instrument with 300 kV accelerating voltage equipped with 2k×2k OriusTM 833 SC200D Gatan CCD camera. Scanning electron microscope (SEM) observations were performed using JEOL JSM-6480 instrument with accelerating voltage of 20 kV equipped with the Energy Dispersive X-ray Spectroscopy (EDAX) detector from IXRF.

RESULTS AND DISCUSSION

Analysis of FTIR Spectra

FTIR measurements were carried out to identify the possible biomolecules responsible for capping and efficient stabilization of the ZnS nanoparticle. For comparison, the spectra of pure ZnS (A0) and capped sample ZnS (A4) recorded in the range of 4000-400 cm^{-1} are presented in Fig. 1. In the higher energy area for pure A0, the peak at 3350.9 cm^{-1} is quite broad and strong which might be assigned to O-H stretching of absorbed water on the floor of ZnS. The peak at 1622 cm^{-1} is assigned to N-H deformation (Amide – II band). The peaks at 771, 623 and 418 cm^{-1} which have been attributed to vibration of Zn-S bond [30]. The slight variation in the peak for capped ZnS nanoparticles are observed (Table 2) which indicates the interaction of biomolecules present in the extract with the surface of prepared samples. The new peak appeared at 1219 cm^{-1} for capped ZnS nanoparticles may be assigned to vibration C- N bond (Amide-III band) [20, 31] which

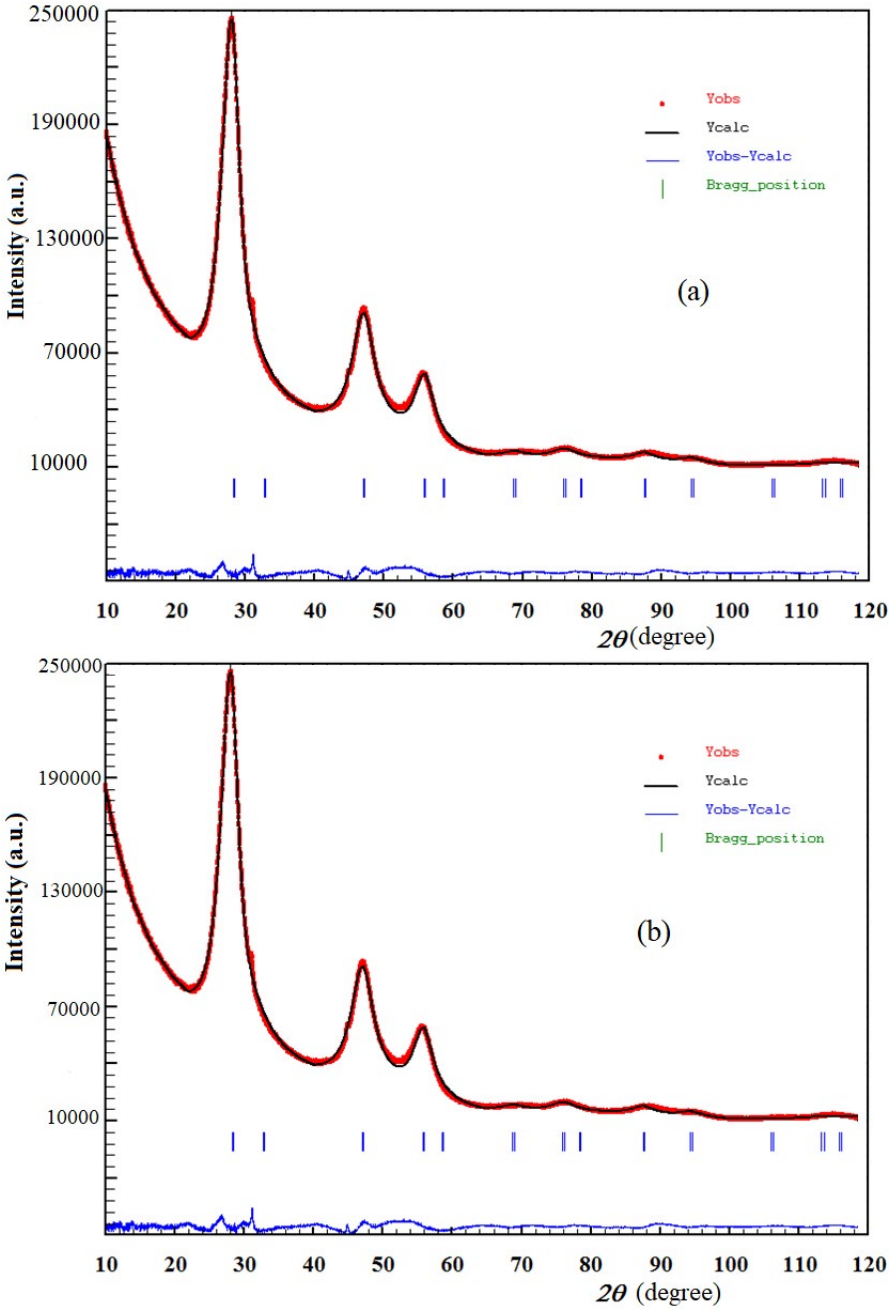

Fig. 2. Powder XRD patterns: (a) pure ZnS, A0, (b) 10mlNLE capped ZnS, A2.

indicates that the protein molecules in the extract is responsible for capping the ZnS nanoparticles. Table 2 summarizes the bands observed in the FTIR spectra of the synthesized ZnS samples.

Powder XRD analysis

Powder XRD patterns of all the ZnS samples were obtained at room temperature and analysed by Rietveld refinement method using Fullprof software. Figs. 2(a) and 2(b) show the XRD patterns of A0 and A2 as the representative results. The Bragg planes are indicated by the vertical line (I), the difference between the observed and calculated intensities is indicated

Table 3: Values of lattice parameters (a, b, c), unit cell volume (V), lattice spacing (d), mean crystallite size (D), dislocation density (δ) and strain (**εstrain**) estimated from powder XRD analysis of ZnS samples.

Sample	a = b = c (A^0)	V (A^{03})	d (A^0)	D (nm)	δ x10^{-16} (lines/m^2)	ε_{strain} x10^{-3}
A0	5.4363	160.66	3.138	1.8	13.14	51.74
A1	5.4566	162.47	3.1504	1.6	19.31	62.31
A2	5.4531	162.16	3.1483	1.8	19.31	62.23
A3	5.4636	163.09	3.1544	1.7	19.32	62.39
A4	5.4640	163.13	3.1546	1.6	26.26	72.75

by (-). A good agreement between the observed and simulated intensity is evident. The Rietveld refinement confirmed that the crystal system of the synthesized ZnS sample is cubic with space group F-43m. Three major peaks are observed at around 28.42^0, 47.27^0 and 56.1^0 for sample A0. With increasing NLE amount a consistent change in these diffraction angles has been noted. The positions of these major peaks correspond to the cubic lattice structure of ZnS [JCPDS card no. 00-065-0723] and can be assigned to the (hkl) planes (111), (220) and (311) accordingly. No diffraction peaks from other crystalline forms or impurities are detected which indicate that the obtained ZnS nanoparticles are of high purity. The lattice parameters estimated are summarized in Table 3. Broadening of the XRD patterns indicates the nanocrystalline nature of the samples.The mean crystallite size has been calculated following the Scherrer equation [32].

$$D = \frac{K\lambda}{\beta Cos\theta} \quad (1)$$

where D is the crystallite size, *K* is the geometric factor (0.9), λ is the X-ray wavelength (1.541A^0), β is the full width at half maximum (FWHM) of the diffraction peaks (in radian) and θ is the diffraction angle. The average crystallite size estimated is presented in Table 3.

The interplanar spacing 'd' and lattice constant 'a' are calculaed using the equation (2) and (3), respectively given below:

$$d_{hkl} = \frac{n\lambda}{2Sin\theta} \quad (2)$$

$$a = d\sqrt{(h^2 + k^2 + l^2)} \quad (3)$$

where h, k and l are the Miller indices for the respective planes.The calculated lattice constants are slightly different from the bulk value (5.42 A^0) [12] which indicates the presence of strain in the samples. Further the volume of the unit cell is estimated according to the formula ($V = a^3$), where a is the lattice parameter of the sample. The average strain (ε_{strain}) of the samples is estimated using the Stokes-Wilson equation [17]

$$\varepsilon_{str} = \frac{\beta}{4tan\theta} \quad (4)$$

where β is the FWHM and θ is the diffraction angle. The strain in turn is related to the dislocation developed in the crystal where the dislocation density (δ) represents the amount of defect in the sample which is determined by the formula suggested by Williamson and Smallman [33]

$$\boldsymbol{\delta} = 1/D^2 \quad (5).$$

All parameters estimated using powder XRD pattern for the synthesized samples are compared in Table 3. It is clear from this table that the average crystallite size decreases with increase in the amount of extract. This decrease in crystallite size in turn leads to increase of dislocation density and average strain. The increase of extract concentration may decrease the nucleation of the particles, which reduces the grain growth of the nanoparticles.

Analysis of SEM, EDAX and TEM results

The morphology of the samples has been studied by SEM. The SEM images for A0 and A2 are compared in Figs. 3(a) and 3(b). From the SEM images no significant effect on the surface morphology of the particles could be detected. However, considering the SEM images of all the samples, it is noted that the particles are agglomerated. The agglomeration as well as

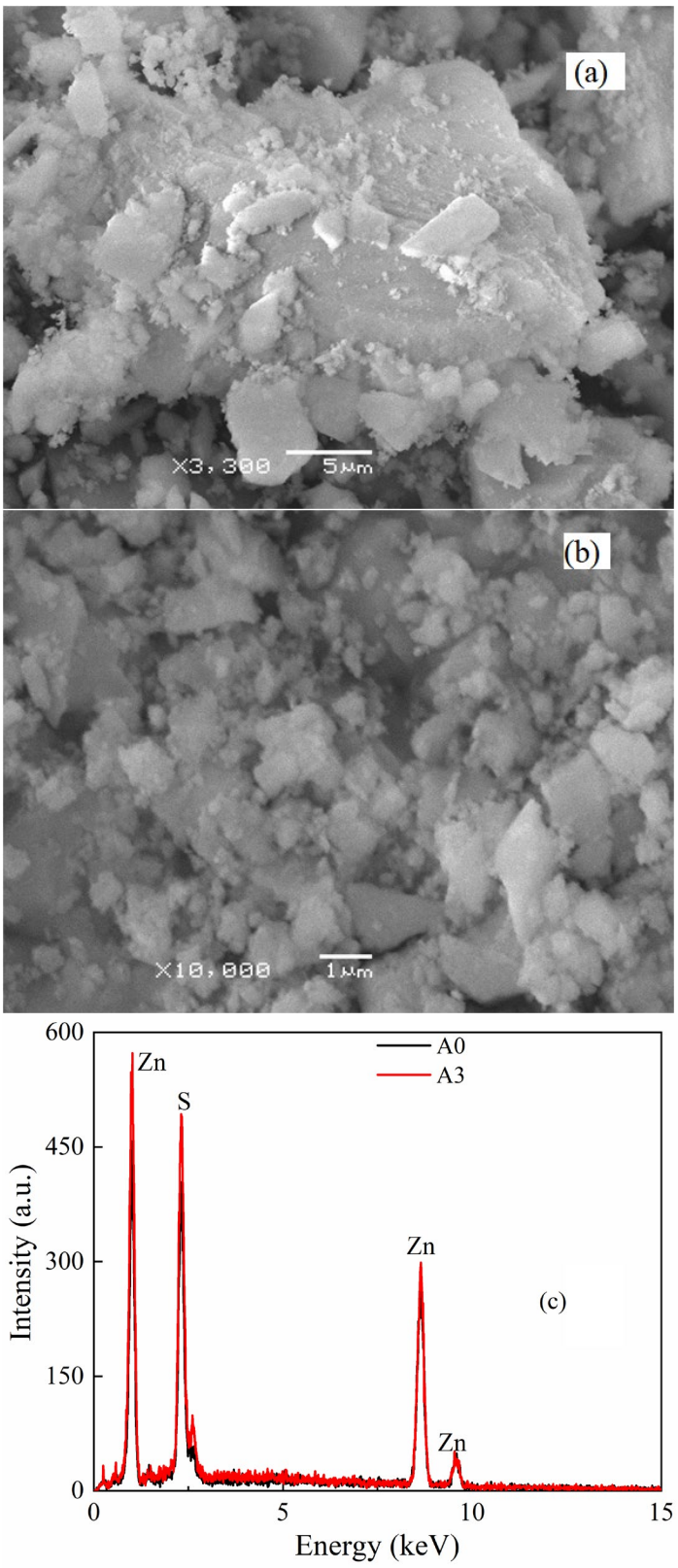

Fig. 3. SEM images: (a) pure ZnS, A0, (b) 2.5mlNLE capped ZnS, A1. (c) EDAX spectra of pure ZnS, A0 and 2.5ml NLE capped ZnS, A3.

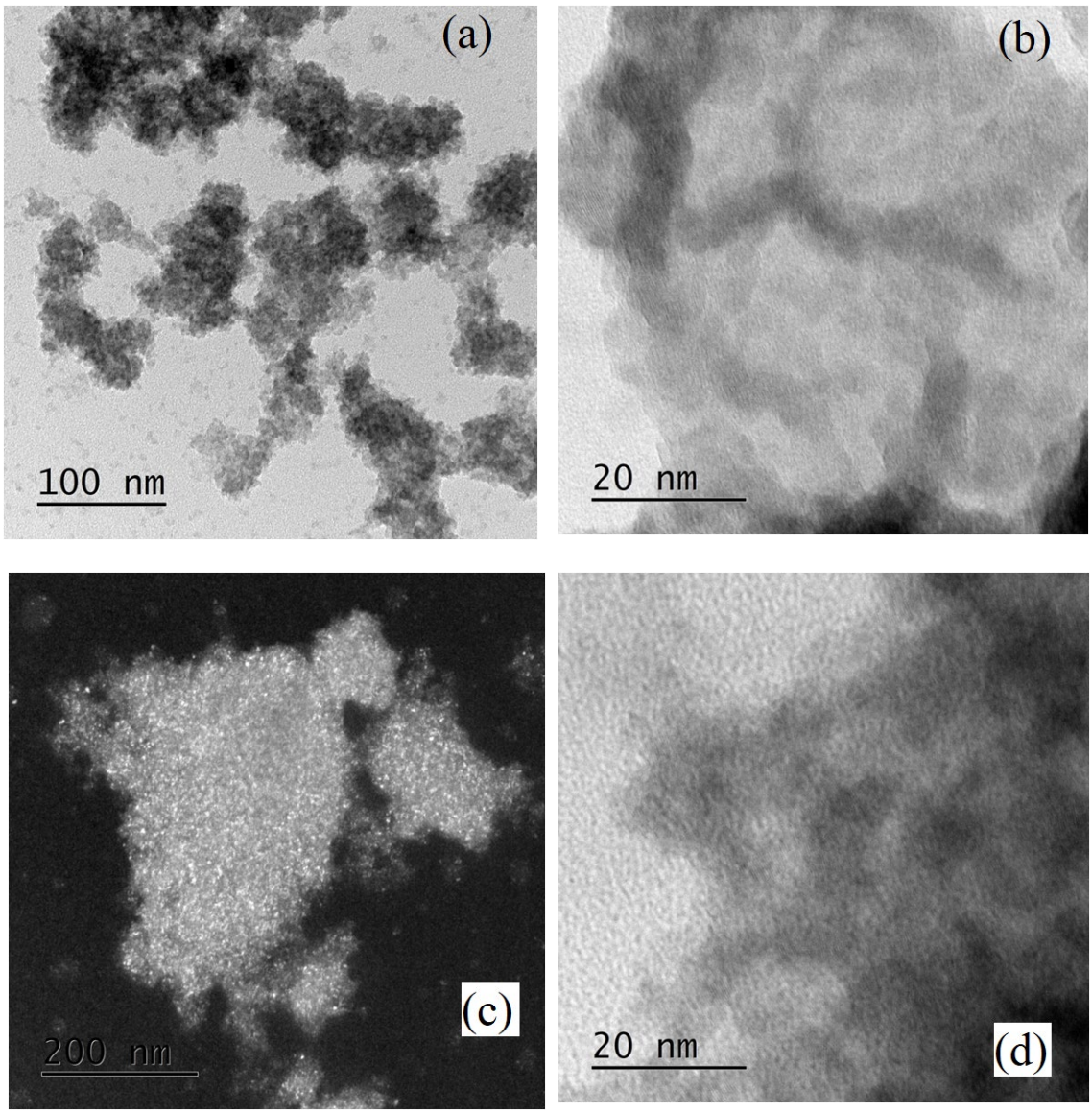

Fig. 4. TEM images at different resolutions: (a) pure ZnS, A0 (lower resolution); (b) pure ZnS, A0 (higher resolution); (c) 5ml NLE capped ZnS, A2 (lower resolution); (b) 5ml NLE capped ZnS, A2 (higher resolution).

particle size decreases with the increase of NLE amount. With higher the amount of NLE, the more almost spherical shaped nanoparticles were obtained. However, the actual size could not be estimated by SEM due to the limitation of the resolution of the instrument. EDAX spectra of the synthesized samples were obtained from the selected regions of the corresponding SEM images. Fig. 3(c) shows the EDAX spectra of A0 and A3. The analysis of the spectra confirms the characteristic peak signals due to the presence of elements Zinc (Zn) and sulphur (S) in the samples.

Particle size of the synthesized ZnS samples were studied with help of TEM. Figs.4(a), 4(b), 4(c) and 4(d) show the TEM images of A0 and A2 at two different resolutions. These images show that the samples are composed of agglomerated tiny particles. The particle size distrubution of all ZnS samples was obtained from the histograms obtained using ImageJ software. Two representative results for A0 and A2 are shown in Figs. 5 (a) and 5(b) where the average particle

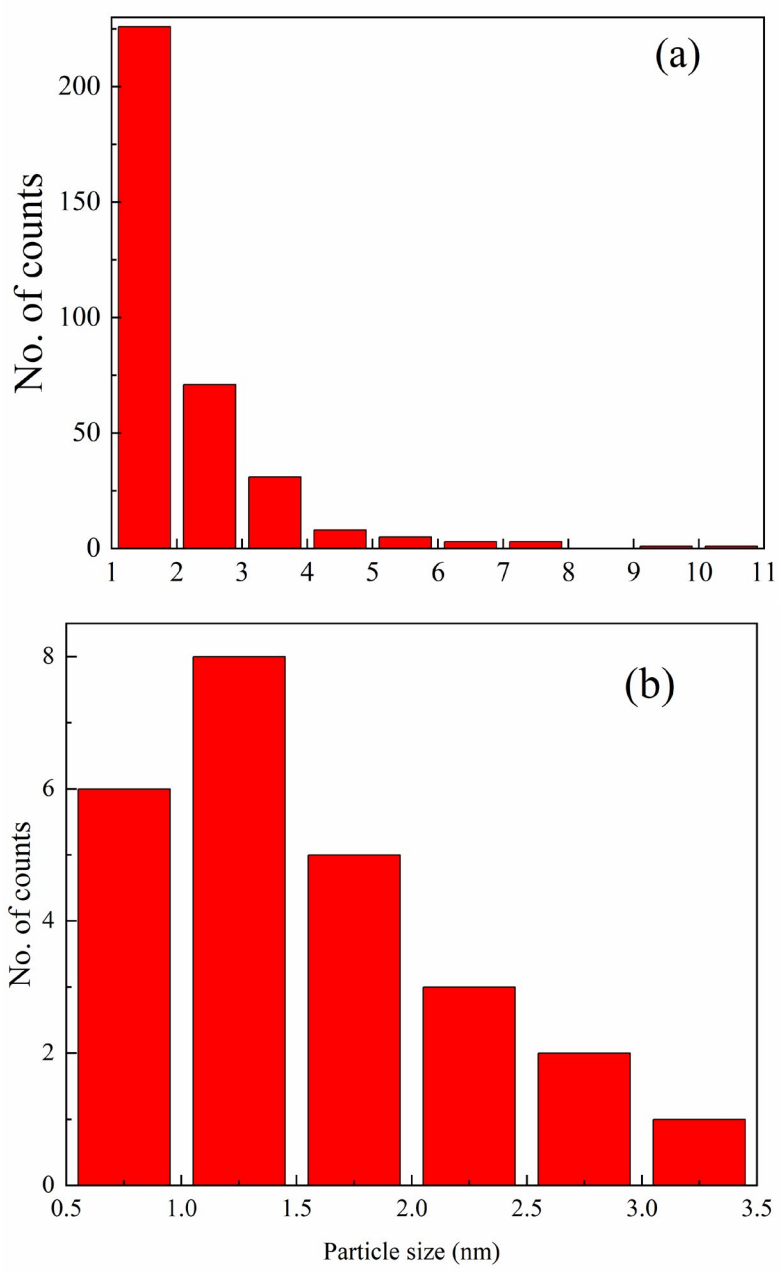

Fig. 5. Particle size histogram: (a) pure ZnS, A0; (b) 5ml NLE capped ZnS, A2.

size of A0 and A2 are found to be ~1.5 and ~1.25 nm, respectively. The particle sizes thus estimated from TEM study for all samples are in agreement with those obtained from the XRD analysis. The Selected Area Electron Diffraction (SAED) patterns were recorded from the selected TEM images for all the ZnS samples and the patterns (Figs. 6(a) and 6(b) for A0 and A2) show the concentric rings indicating the diffraction planes of ZnS crystals. No significant difference in the SAED patterns for different samples has been recorded.

Analysis of UV-Visible absorption spectra

UV-Visible spectra of all ZnS samples were obtained. The insert of Fig. 7 shows the UV-Visible spectrum of ZnS sample A0 as the representative

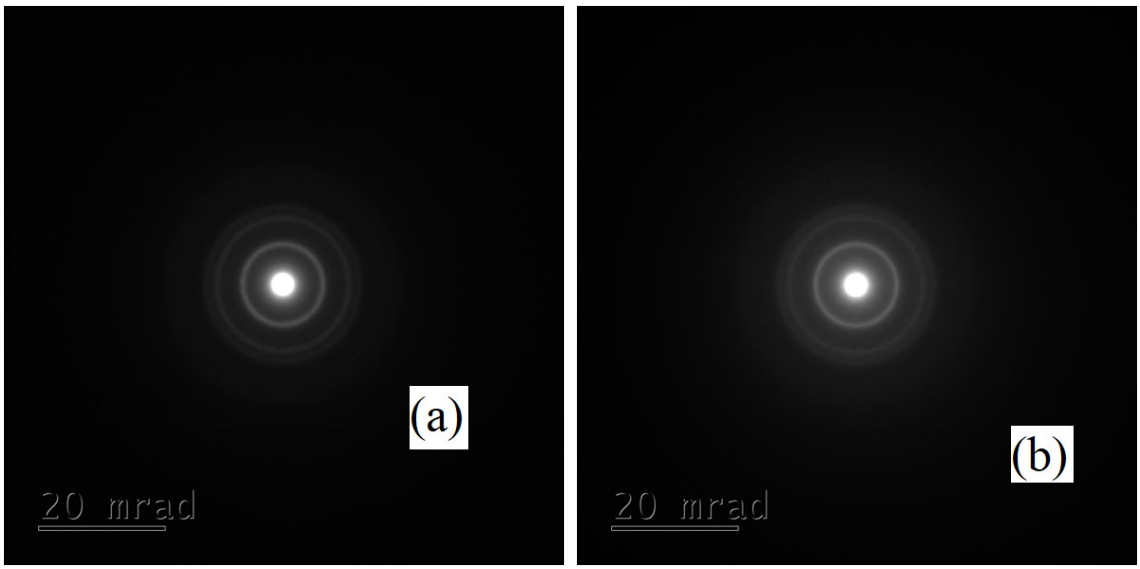

Fig. 6. The SAED patterns: (a) pure ZnS, A0; (b) 5ml NLE capped ZnS, A2.

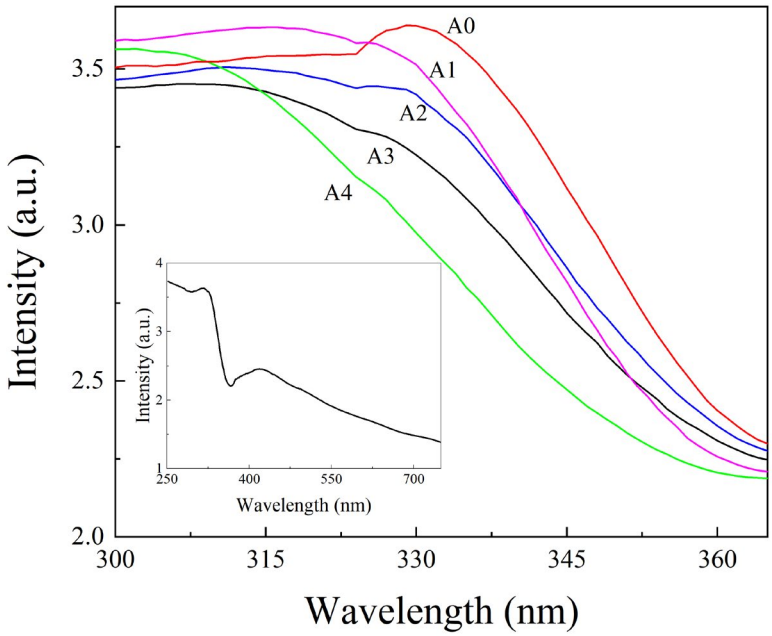

Fig. 7. UV-Visible spectra of all ZnS samples in a reduced wavelength range. The insert shows the UV-Visible spectra obtained for A0.

plot whereas the spectra obtained for all samples in a reduced wavelength range is presented in Fig. 7. From the spectra, it is found that there is a strong absorption at 329 nm for A0 and at 316, 311, 308 and 302 nm for capped ZnS samples - A2, A3, A4 and A5,respectively suggesting a blue shift compared to the bulk ZnS. This blue shift may be attributed to the quantum confinement effect of nanoparticles. The band gap of these quantum dots may be assessed by theoretical, semi-empirical and empirical models. Using the direct formula [34], the band gap is given by

$$E_g(eV) = hc/\lambda_{max}(nm) = 1241/\lambda_{max}(nm) \quad (6)$$

Table 4: Values of absorption maximum (in UV-Vis spectra), band gap energy, particle size derived using eqns. (7), (8) and (1) for ZnS samples.

Sample	λ_{max} (nm)	E_g (eV)	D_p^7 (nm)	D_p^8 (nm)	D_{xrd} (nm)
A0	329	3.77	1.75454	1.73749	1.8
A1	316	3.93	1.66584	1.565	1.6
A2	311	3.99	1.63407	1.51058	1.8
A3	308	4.03	1.61558	1.48114	1.7
A4	302	4.11	1.57985	1.42953	1.6

The band gap energies corresponding to the absorption edge observed for the samples A0, A1, A2, A3 and A4 are estimated to be 3.77 eV, 3.93 eV, 3.99 eV, 4.03 eV and 4.11 eV, respectively. These band gap values are higher than the bulk value (3.68 eV) for ZnS with cubic structure confirming the blue shift observed in the UV-Visible spectrum [35]. Several extracts have been used for synthesis of ZnS by green chemical method. The optical band gap values obtained from the UV-Visible spectral study of some of the green-synthesized ZnS nanoparticles are as follows: moringa oliefera leave (4.12 eV) [11]; acalypha indica (3.89 eV) [12]; curcuma longa (3.89 eV) [12]; elaeocarpus floribundus leave (3.8-4.1 eV) [13]; banana peel (4.36–4.59 eV) [14]; honey (4.08) [15]; ostreatus mushroom (4.68–4.75) [17]; agaricus biosporus mushroom (4.90–5.30 eV) [18]. These values are quite comparable with the presently observed values.

The average size of the ZnS nanocrystals can be estimated using the empirical model published in the literature [36]. The diameter of the nanoparticle is correlated with the absorption wavelength edge and the size of the nanoparticle can be estimated using the equation (7) as

$$2R = \frac{0.1}{\left(0.1338 - 0.0002345\lambda\right)}\left(nm\right) \qquad (7)$$

where R is the radius of the nanoparticle and λ is the absorption wavelength edge. Using the observed absorption wavelength edge values, the diameters of the ZnS nanoparticles are calculated and tabulated in Table 4 as D_p^7.

Size of the ZnS nanoparticle was also evaluated using the following empirical formula [37]

$$D = -6.65\times10^{-8}\lambda^3 + 1.96\times10^{-4}\lambda^2 - 9.24\times10^{-2}\lambda + 13.29 \qquad (8)$$

where λ is the position of the low-energy absorption maxima in the UV-Visible spectrum, and the estimated values are shown in Table 4 as D_p^8. From Table 4, it is clear that the particle size values estimated using the UV-Visible spectral data are in good agreement with those obtained from powder XRD analysis (equation 1).

The variations of the particle size determined by equations (7), (8) and (1) with the NLE amount are shown in Fig. 8. The lines are the fit of the experimental data with following mathematical relations:

equation (*7*): $D_p^7 = \sum_{n=0}^{2} a_n (NLE)^n$, $a_0 = 1.731$, $a_1 = -0.024$, $a_2 = 9.728\times10^{-4}$;

equation (*8*): $D_p^8 = b_0 + b_1\exp\{-(NLE)/b_2)\}$, $b_0 = 1.427$, $b_1 = 0.306$, $b_2 = 3.540$;

equation (*1*): $D_{XRD} = a + b(NLE)$, $a = 1.76$, $b = -0.012$.

The variation of the optical band gap (E_g) with the amount of particle size obtained following equation (7) and (8) are shown in Fig. 8 as an insert. The E_g vs. particle size data can be well-fitted with the following linear relation:

$E_g = a\text{-}b(Particle\ Size)$, $a = 7.146$, $b = 1.924$ for D_p^7 and $a = 5.619$, $b = 1.076$ for D_p^8.

Effect of extract

From the observed UV-Visible absorption spectra it is seen that the band gap energy values linearly increase with the increasing NLE amount with a concomitant shrinking of the ZnS nanoparticle size. The absorption maximum is shifted to the shorter wavelength side with decreasing particle size leading to a corresponding increase in the confinement energies owing to downward and upward movements of the valence

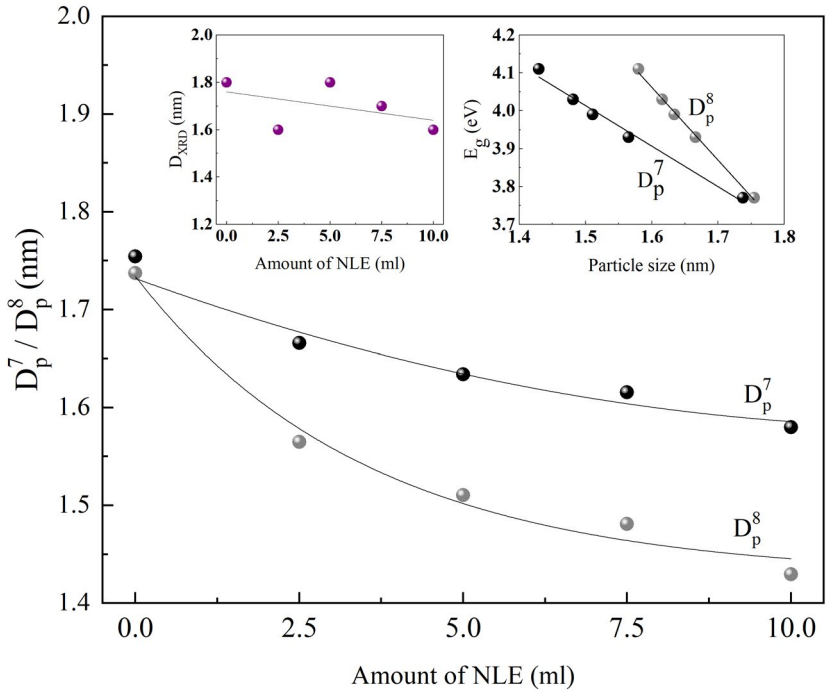

Fig. 8. Variation of particle size estimated by equation (7) and equation (8) with the amount of NLE used for synthesis of ZnS nanoparticle. Similar variation for the particle size estimated by equation (1) (D_{XRD}) with the amount of NLE is shown as left insert of Fig. 8. The solid lines are the fits of the experimental data with mathematical relations. The right insert shows the dependence of the band gap energy (E_g) on the particle size derived by using equation (7) and equation (8). The straight lines present the linear dependence of E_g with the amount of NLE. All fitting results are described in the text.

and conduction bands, respectively, and thus widening the band gap of the ZnS semiconductor nanocrystals. This results into a blue-shift of the excitation energy of the semiconductor. Based upon the cohesive energy, Sing et al. [35] has proposed a theoretical model for size- and shape-dependent band gap energy of semiconductor nanomaterials. According to this model, the band gap energy should increase with the decreasing particle size of the semiconductor nanomaterials following the relation given by

$$E_g(nano) = E_g(bulk)\,(1 + 2d/D) \qquad (9)$$

where d and D being the diameter of an atom and the spherical nanoparticle, respectively. Presently observed results, as shown in Fig. 8, exhibit a linear increase in the band gap energy of the NLE capped ZnS nanoparticle with decreasing particle size which is in complete agreement with the proposed model. The estimated band gap energy values for the synthesized nanoparticle are higher when compared to typical band gap of bulk ZnS (3.68 eV at 300K). The band gap variation is due to presence of trap-levels within the band gap [13]. The increase in the band gap and shift in the electron transition to higher energies with decreasing particle (quantum dot) size is the combined effect owing to the enhancement in surface/volume ratio and accompanied increase in the oscillation strength of the nanocrystals induced by the quantum size effect [38]. The quantum confinement effect allows one to tune the emission and excitation wavelengths of nanoparticles by tuning particle size.

CONCLUSION

ZnS nanoparticle has been synthesized by cost-effective green chemical method using the extract of Neem leaf. The nanoparticles were characterized by different physical techniques like FTIR, powder XRD, SEM, EDAX, TEM and UV–Visible spectroscopy. FTIR analysis confirmed that the protein molecules in the extract are responsible for capping of the ZnS nanoparticles. Powder XRD analysis confirmed the formation of pure cubic

phase of ZnS nanocrystals. It is found that the average crystallite size decreases with increase in the amount of extract used. The decrease in crystallite size led to the increase in dislocation density and average strain in the nanocrystals. The particle size was directly estimated by using TEM and compared with that calculated using UV-Visible spectral data, and in all cases the particle sizes were in very good agreement with that observed by powder XRD analysis. The particle sizes of the synthesized ZnS lie in the range expected for quantum dots and the particle size of ZnS depends on the amount of extract used in the synthesis. The amount of extract also significantly controls the optical band gap of the semiconducting nanoparticle. In conclusion, Neem leaf extract capped potentially applicable ZnS nanoparticle of quantum dot size is prepared by green chemical method and physically characterized.

The true mechanism of the formation of green-synthesized nanoparticle is not yet clear, but from the literature it is found that the biomolecules, either individually or in combination, act as the capping / reducing agent in the chemical synthesis [39, 40]. Several factors, like reaction temperature, particle size, pH and concentration of the extract may affect the synthesis. What generally observed as possible reasons for nanoparticle size variations are (i) the concentration of polyphenols present playing the key role in reducing/capping performance, and (ii) the pH range leading to the agglomeration by over nucleation at low pH whereas instability of nanoparticle at high pH. In this light, our future research will be directed in exploring these features in controlling size of nanoparticle synthesized by green synthetic method.

CONFLICT OF INTEREST

The authors declare that they have no competing interests.

REFERENCES

[1] Fang X., Zhai T., Gautam U. K., Li L., Wu L., Bando Y., Golberg D., (2011), ZnS nanostructures: From synthesis to applications. *Prog. Mater. Sci.* 56: 175–287.

[2] Pourahmad A., (2015), Ion exchange growth of Zinc Sulfide quantum dots in aqueous solution. *Int. J. Nano Dimens.* 6: 83-88.

[3] Kumar N., Purohit L. P., Goswami Y. C., (2016), Spin coating of ZnS nanostructures on filter paper andtheir characterization. *Phys. E*. 83: 333–338.

[4] Sreekala G. N., Abdullakutty F., Beena B., (2019), Green synthesis, characterization and photo catalytic degradation efficiency of trimanganese tetroxide nanoparticle. *Int. J. Nano Dimens*. 10: 400-409.

[5] Zhou J., Sheng Z., Han H., Zou M., Li C., (2012), Facile synthesis of fluorescent carbon dots using watermelon peel as a carbon source. *Mater. Lett.* 66: 222–224.

[6] Bankar A., Joshi B., Ravi Kumar A., Zinjarde S., (2010), Banana peel extract mediated novel route for the synthesis of silver nanoparticles. *Colloids Surf.* 368: 58–63.

[7] Bankar A., Joshi B., Ravi Kumar A., Zinjarde S., (2010), Banana peel extract mediated synthesis of gold nanoparticles. *Colloids Surf. B*. 80: 45–50.

[8] Zhou G. J., Li S. H., Zhang Y. C., Fu Y. Z., (2014), Biosynthesis of CdS nanoparticles in Banana peel extract. *J. Nanosci. Nanotechnol.*14: 4437–4442.

[9] Sathishkumar M., Saroja M., Venkatachalam M., (2017), Characterization and antimicrobial activity of green synthesized zinc sulphide nanoparticles using plant extracts of phyllanthus niruri. *Int. J. Chem. Sci.* 15: 123-130.

[10] Satishkumar M., Saroja M., Venkatachalam M., Parthasarathi G., Rajamanickam A. T., (2017), Biosynthesis and characterization of zinc sulphide nanoparticles using leaf extract of tridaxprocumbens. *Orient. J. Chem.* 33: 903-909.

[11] Sur U. K., Ankamwar B., (2016), Optical, dielectric, electronic and morphological study of biologically synthesized zinc sulphide nanoparticles using *moringa oleifera* leaf extract and quantitative analysis of chemical components present in the leaf extract. RSC Adv. 6: 95611-95619.

[12] Satishkumar M., Saroja M., Venkatachalm M., (2019), Acalypha and curcuma longa plant extracts mediated ZnS nanoparticles. *Mat. Sci. Res. Ind.* 16: 174-182.

[13] Senapati U. S., Sarkar D., (2015), Structural, spectral and electrical properties of green synthesized ZnS nanoparticles using elaeocarpus floribundus leaf extract. *J. Mater. Sci: Mater. Electron.* 26: 5783–5791.

[14] Bisauriya R., Verma D., Goswami Y., (2018), Optically important ZnS semiconductor nanoparticles synthesized using organic waste banana peel extract and their characterization. *J. Mater. Sci: Mater. Electron.* 29: 1868–1876.

[15] Esakkiammal A., Malathi A., Ujjal K. S., Balaprasad A., (2018), Honey mediated green synthesis of photoluminiscent ZnS nano/micro particles. *Res. Med. Eng. Sci.* 3: 214-219.

[16] Satishkumar M., Saroja M., Venkatachalam M., (2017), Green synthesis, characterization and antimicrobial activity of ZnS using syzygium aromaticum extracts. *Int. J. Chem. Tech. Res.*10: 443-449.

[17] Senapati U. S., Sarkar D., (2014), Characterization of biosynthesized zinc sulphide nanoparticles using edible mushroom Pleurotuss ostreatu. *Ind. J. Phys.* 88: 557–562.

[18] Senapati U. S., Jha D. K., Sarkar D., (2015), Structural, optical, thermal and electrical properties of fungus guided biosynthesized zinc sulphide nanoparticles. *Res. J. Chem. Sci.* 5: 33-40.

[19] Bai H. J., Zhang Z. M., Gong J., (2006), Biological synthesis of semiconductor zinc sulfide nanoparticles by immobilized rhodobacter sphaeroides. *Biotech. Letts*. 28: 1135–1139.

[20] *Malarkodi C., Rajeshkumar S., Paulkumar C., Vanaja M., Gnanajobitha G., Annadurai G., (2014),* Biosynthesis and antimicrobial activity of semiconductor nanoparticles against oral pathogen. *Bioinorg. Chem. Appl. Article ID 347167, 10* pages.

[21] Chopra R. N., Nayer S. L. and Chopra I. C., (1956), Glossary

of indian medicinal plants, CSIR, New Delhi.
[22] Biswas K., Chattopadhyay I., Banerjee R. K., Bandyopadhyay U., (2002), Biological activities and medicinal properties of neem (Azadirachtaindica). *Curr. Sci*. 82: 1336–1345.
[23] Tiwari V., Darmani N. A., Yue B. Y., Shukla D., (2010), In vitro antiviral activity of neem (*Azardirachta indica L*.) bark extract against herpes simplex virus type-1 infection. *Phytother. Res*. 24: 1132–1140.
[24] Mahapatra S., Jeffrey Karnes R., Holmes M. W., Young C. Y. F., Cheville J. C., Kohli M., Klee E. W., Tindall D. J., K. V., (2011), Novel molecular targets of Azadirachta indica associated with inhibition of tumor growth in prostate cancer. *AAPS J*. 13: 365–377.
[25] Gupta S., Kataria M., Gupta P. K., Murganandan S., Yashroy R. C., (2004), Protective role of extracts of neem seeds in diabetes caused by streptozotocin in rats. *J. Ethnopharmacol.* 90: 185–189.
[26] Banerjee P., Satapathy M., Mukhopahayay A., Das P., (2014), Leaf extract mediated green synthesis of silver nanoparticles from widely available Indian plants: synthesis, characterization, antimicrobial property and toxicity analysis. *Bioresources and Bioprocessing*. 1: 1-10.
[27] Santoshkumar J., Rajeshkumar S., Venkatkumar S., (2017), Phyto-assisted synthesis, characterization and application of gold nanoparticles–A review. *Biochem. Biophys. Rep.* 11: 46–57.
[28] Verma A., Mehata M. S., (2016), Controllable synthesis of silver nanoparticles using Neem leaves and their antimicrobial activity. *J. Rad. Res. Appl. Sci.* 9: 109-115.
[29] Singh A., Neelam Kaushik M., (2019), Physicochemical investigations of zinc oxide nanoparticles synthesized from *azadirachta indica (*neem) leaf extract and their interaction with calf-thymus DNA. *Result in Phys.* 13: 102168-102177.
[30] Sobia D., Mohammad S., Azhar I., (2015), Synthesis of zinc sulphide nanostructures by co- precipitation: Effect of doping on electro-optical properties. *Kenkyu J. Nanotech. Nanosci.*1: 34-39.
[31] Ramteke G. G., Lanje A. S., Pimpalshende D. M., (2018), Structural and optical performance of ZnS nanoparticles synthesized via chemical route. *Int. J. Sci. Res. Phys. Appl. Sci.* 6: 69-74.
[32] Cullty B. D., (1956), Elements of x-ray diffraction, Addison-Wesley, Reading, MA, p.99.
[33] Dhanam M., Kavitha B., Velumani S., (2010), An investigation on silar Cu($In_{1-x}Al_x$)Se_2 thin films. *Mater. Sci. Eng. B.* 174: 209-215.
[34] Pawar R. R., Bhavsar R. A., Sonawane S. G., (2012), Structural and optical properties of chemical bath deposited Ni doped Cd-Se thin films. *Ind. J. Phys.* 86: 871-876.
[35] Singh M., Goyal M., Devlal K., (2018), Size and shape effects on the band gap of semiconductor compound nanomaterials. *J. Taibah Univ. Sci.* 12: 470-475.
[36] He R., Qian X., Yin J., Xi H., Bian L., Zhu Z., (2003), Formation of monodispersed PVP-capped ZnS and CdS nanocrystals under microwave irradiation. *Colloid. Surf*. *A.* 220: 151- 157.
[37] Borovaya M., Pirko Y., Krupodorova T., Naumenko A., Blume Y., Yemets A., (2015), Biosynthesis of cadmium sulphide quantum dots by using pleurotus ostreatus (Jacq.) P. Kumm. *Biotech. Biotech. Equip.* 29: 1156-1163.
[38] Ashcroft N. W., Mermin N. D., (1976), Solid state physics, Sanders College Publishing, Forth Worth, 320-340.
[39] Huang L., Weng X., Chen Z., Megharaj M., Naidu R., (2014), Green synthesis of iron nanoparticles by various tea extracts: Comparative study of the reactivity. *Spectrochim. Acta A. Mol. Biomol. Spectrosc.* 130: 295–301.
[40] Choi Y., Choi M. J., Cha S. H., Kim Y. S., Cho S., Park Y., (2014), Catechin-capped gold nanoparticles: green synthesis, characterization, and catalytic activity toward 4-nitrophenol reduction. *Nanoscale Res. Lett.* 9: 1–8.